IEEE Access
Multidisciplinary | Rapid Review | Open Access Journal

Received September 26, 2021, accepted October 29, 2021, date of publication November 2, 2021,
date of current version November 10, 2021.

Digital Object Identifier 10.1109/ACCESS.2021.3124972

Ascent Guidance Based on Onboard Trajectory Regeneration for Vehicles With a Combined Cycle Engine

XIANGJI TANG, ZHAOTING LI, AND HONGBO ZHANG
College of Aerospace Science and Engineering, National University of Defense Technology, Changsha 410073, China
Corresponding author: Hongbo Zhang (zhanghb1304@nudt.edu.cn)

ABSTRACT For a vehicle with a combined cycle engine, an ascent guidance method based on onboard trajectory regeneration is proposed to meet the requirements of adaptability and robustness. This method combines onboard trajectory planning with reference trajectory tracking and modifies the computational model. In the onboard trajectory planning, a hierarchical receding horizon optimization is developed to update the reference trajectory depending on the current state. Further, the optimization problem subject to multiple constraints is solved by an improved segmented pseudospectral method, in which a recursive initialization strategy is introduced to improve the computational efficiency for onboard application. In reference trajectory tracking, the active disturbance rejection control theory is used to improve the robustness of the tracking process. Based on the theory, an extended state observer for the multi-input and multi-output system is designed to estimate the state and the disturbance. Then, the trajectory tracking law is derived by linearizing the model with dynamic compensation. Besides, the scale factors of the dynamic system are defined to compensate for the uncertainty of the model, and an online estimation method is used to identify the parameters. Numerical simulation validates the efficiency of the proposed method.

INDEX TERMS Onboard trajectory regeneration, ascent guidance, combined cycle engine, active disturbance rejection control.

I. INTRODUCTION

The vehicle with a combined cycle engine is among the most promising developments in aerospace engineering [1]–[5]. The vehicle can be used for space transportation in the future and is superior to traditional launch vehicles [6]. The air-breathing engine aspirates oxygen from the atmosphere to consume less oxidizer. Therefore, the vehicle can maintain hypersonic flight with less fuel compared to traditional launch vehicles. In addition, it has better reusability and higher mission flexibility [7]. The vehicle used in this study is propelled by a turbine-based combined cycle (TBCC), and it can take off horizontally.

The ascent guidance of a vehicle with a combined cycle engine poses considerable challenges. The strong nonlinear coupling among aerodynamic, propulsion, and flight conditions, as well as the different dynamic characteristics of engine modalities, makes it more difficult to generate the guidance commands. Additionally, the guidance method needs to have strong adaptability to handle the uncertainty and changes in the complex system and external conditions. Moreover, the guidance system must also be quite robust as the ascent trajectory is considerably sensitive to disturbances.

The conventional guidance method is to track the reference trajectory [8]–[12]. In such an approach, the reference trajectory is generated offline. The design of the nominal flight profile is important, and the trajectory design is usually converted into an optimization problem. The methods for numerical trajectory optimization may be broadly classified as ''indirect method'' and ''direct method'' [13]. The indirect method transforms the trajectory optimization problem into a two-point-boundary-value problem (TPBVP) based on Pontryagin's Minimum Principle [14]. The direct method converts the continuous problem into a nonlinear programming problem by direct discretization. Whereas, the adaptive capability of the tracking guidance is not enough to handle the control saturation and contingencies, and it also does not possess the robustness necessary to cope with significant off-nominal conditions and model uncertainty.

The associate editor coordinating the review of this manuscript and approving it for publication was Haibin Sun.

With the advance in onboard computation, fast onboard trajectory optimization has become a research focus [15]–[19]. Onboard optimization can generate the prospective open-loop control based on the current state and then guide the vehicle. Zhang *et al*. [20] use a direct method to optimize the trajectory and successively generate open-loop suboptimal controls. Lu *et al*. [21] solve the trajectory optimization problem by an indirect method, and then generate the guidance commands that are based on correcting the reference trajectory to satisfy the optimality condition. Onboard optimization requires high computation speed, and it is challenging to solve the optimization problem with complex models. Therefore, an appropriate algorithm and proper simplification of the model is needed. Moreover, Zhou *et al*. [22] generate a database of trajectories by offline trajectory optimization, and then, based on the current states and database, the guidance commands are updated by a neural network. This is a new perspective for the ascent guidance of the vehicle with a combined cycle engine.

This paper presents another ascent guidance scheme for the vehicle with a combined cycle engine. The guidance method employs receding horizon optimization, active disturbance rejection control (ADRC), and model modification to address the deficiencies of traditional trajectory tracking guidance. Firstly, a hierarchical receding horizon optimization is developed to adaptively update the reference trajectory according to the state feedback which implies disturbance information. The segmented pseudo-spectral method is used to solve the trajectory optimization problem, which is a direct method. For onboard application, recursive initialization of the pseudospectral optimization method is used to improve computational efficiency. Then, the trajectory tracking law is derived based on the ADRC theory, which estimates the ''total disturbance'' based on the extended state observer and linearizes the model with dynamic compensation. It can handle the deviation caused by uncertainties and external disturbance. Finally, to further improve the adaptability and robustness of the method, parameter estimation is used to modify the model.

The remainder of this paper is organized as follows: Section II presents the equations of motion, models of the engine and aerodynamics, and the trajectory optimization problem. Section III discusses the ascent guidance algorithm. In Section IV, numerical simulations are conducted to validate the efficiency of the guidance method. Section V concludes the work in this paper.

II. PROBLEM FORMULATION

A. ASCENT DYNAMICS

The longitudinal motion of the vehicle is mainly considered in the ascent phase. Assuming a spherical, non-rotating Earth, the equations of motion for a vehicle are given as follows:

$$\begin{cases} \dot{h} = v\sin\theta \\ \dot{s} = vR_e\cos\theta/(R_e + h) \\ \dot{v} = (P\cos\alpha - D)/m - g\sin\theta \\ \dot{\theta} = (P\sin\alpha + L)/(mv) - (g/v - v/(R_e + h))\cos\theta \\ \dot{m} = -K_s\phi_t\rho v C_A S_c \end{cases} \tag{1}$$

where h, s, v, θ, and m denotes altitude, range, velocity, flight path angle, and mass, respectively. α is the angle of attack (AOA), and ϕ_t is the throttle coefficient. g is the local gravitational acceleration, R_e is the radius of the Earth; L and D represent the aerodynamic lift and drag forces, respectively, P is vehicle thrust; ρ is the atmospheric density which is calculated according to [23], K_s is scale coefficient, S_c is capture area, and C_A is the effective area coefficient, which is represented as a function of Mach number and AOA.

The state and the guidance command of the ascent trajectory are denoted as $\boldsymbol{x} = [h,\ s,\ v,\ \theta,\ m]^T$, $\boldsymbol{u} = [\phi_t,\ \alpha]^T$, respectively. In the guidance, the above equations are nondimensionalized to reduce the error in numerical calculation and for better numerical conditions in onboard optimization. Altitude and range are normalized by R_e, and time t is normalized by $\sqrt{R_e/G_0}$,where G_0 is the gravitational acceleration on the Earth's surface. The velocity is normalized by $\sqrt{R_eG_0}$, mass is normalized by m_0, the initial mass of the vehicle, and the forces are normalized by m_0G_0.

The aerodynamic forces are given by the following equations:

$$\begin{cases} L = 0.5\rho v^2 S_{\text{ref}} C_L \\ D = 0.5\rho v^2 S_{\text{ref}} C_D \end{cases} \tag{2}$$

where S_{ref} is the reference area of the vehicle; the lift coefficients, C_L, and the drag coefficients, C_D, are calculated with Mach number and AOA.

The thrust model is as follow:

$$P = K_s\phi_t\rho v C_A S_c G_0 I_{sp} \tag{3}$$

where I_{sp} is the specific impulse, which is a function of Mach number and throttle coefficient. The thrust increases monotonously with the control variable ϕ_t, and Equation (3) indicates the characteristics of the air-breathing propulsion that relates the thrust with the AOA, the velocity, and the environment simultaneously.

The coefficients C_A, C_L, C_D, and I_{sp} are calculated by interpolating the lookup table. These coefficients reflect the complex interactions among the propulsion system, vehicle aerodynamics, flight conditions, and control command. The interpolation data and parameters of the vehicle are taken from [24]. The combined cycle engine includes a turbojet cycle, ramjet cycle, and scramjet cycle. The ranges of the cycles are turbojet, 0–2 Mach number; ramjet, 2–6 Mach number; scramjet, greater than 6 Mach number. It is assumed that the engine would change automatically from one cycle to the next.

B. TRAJECTORY OPTIMIZATION MODEL

The trajectory optimization problem can be described as an optimal control problem, including the performance index, control variables, and constraints. In contrast to the trajectory simulation, the control variables in optimization are selected as the derivative of the AOA and throttle coefficient to limit the change in guidance command. Thus, the extended state

vector $\hat{\boldsymbol{x}} = [h, s, v, \theta, m, \phi_t, \alpha]^T$ in optimization, and the corresponding control $\hat{\boldsymbol{u}} = [\dot{\phi}_t, \dot{\alpha}]^T$.

In the ascent phase, several path constraints are considered:

$$\begin{aligned} \phi_{t,\min} \le \phi_t \le \phi_{t,\max}, \alpha_{\min} \le \alpha \le \alpha_{\max} \\ \dot{\phi}_{t,\min} \le \dot{\phi}_t \le \dot{\phi}_{t,\max}, \dot{\alpha}_{\min} \le \dot{\alpha} \le \dot{\alpha}_{\max} \\ q = 0.5\rho v^2 \le q_{\max} \end{aligned} \tag{4}$$

where q denotes the dynamic pressure.

The boundary conditions at initial time t_0 and terminal time t_f are given as

$$\begin{aligned} h(t_0) = h_0, \quad v(t_0) = v_0, \ \theta(t_0) = \theta_0, \ m(t_0) = m_0 \\ h(t_f) = h_f, \quad Ma(t_f) = Ma_f, \ \theta(t_f) = \theta_f \end{aligned} \tag{5}$$

where Ma denotes the Mach number. The subscript "0" and "f" denote the initial value and terminal value, respectively.

To maximize the transport capacity of the vehicle, the performance index is chosen so as to minimize fuel consumption, which is also equivalent to maximizing the terminal mass. Thus, the optimization problem is given as

$$\begin{aligned} &\min J = -m(t_f) \\ &\text{s.t.} \begin{cases} \dot{\hat{\boldsymbol{x}}}(t) = \boldsymbol{f}(\hat{\boldsymbol{x}}(t), \hat{\boldsymbol{u}}(t)) \\ \Phi(\hat{\boldsymbol{x}}(t_0), \hat{\boldsymbol{x}}(t_f)) = 0 \\ C(\hat{\boldsymbol{x}}, \hat{\boldsymbol{u}}) \le 0 \end{cases} \end{aligned} \tag{6}$$

where $\dot{\hat{\boldsymbol{x}}}(t) = \boldsymbol{f}(\hat{\boldsymbol{x}}(t), \hat{\boldsymbol{u}}(t))$ denotes the dynamic constraints, $\Phi(\hat{\boldsymbol{x}}(t_0), \hat{\boldsymbol{x}}(t_f)) = 0$ denotes the equality boundary constraints, $C(\hat{\boldsymbol{x}}, \hat{\boldsymbol{u}}) \le 0$ denotes the inequality path constraints.

III. ASCENT GUIDANCE ALGORITHM

As shown in Fig. 1, the guidance scheme comprises three parts: onboard trajectory regeneration, reference trajectory tracking, and model modification. The guidance command is generated by tracking the reference trajectory, and the reference trajectory is updated onboard according to the current state. In addition, the models in optimization and tracking control are modified by parameter estimation.

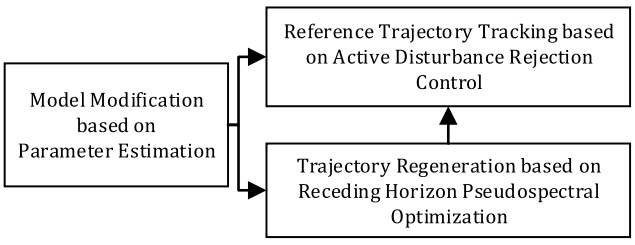

FIGURE 1. Guidance scheme.

A. ONBOARD TRAJECTORY REGENERATION

The hierarchical receding horizon optimization updates the reference trajectory to deal with the disturbance. The new reference trajectory is generated by solving the trajectory optimization problem subject to multi-constraints, and this optimal control problem is solved by the segmented pseudospectral method. The method divides the total time interval into a mesh and discretizes the continuous problem into a nonlinear programming problem (NLP). Then, the discrete optimal solution of the original problem is obtained by iteratively solving the NLP. It can effectively deal with constrained problems and has the potential to solve the optimal control problem quickly. The details of the segmented pseudospectral method are shown in [25].

To improve the efficiency of the segmented pseudospectral method, both the discrete mesh and the iterative solution must be initialized appropriately. The mesh forms the basis of NLP formulation, which is related to the size and characteristics of the transformed NLP. An appropriate mesh can reduce the difficulty of the NLP and also the construction of sequential NLPs. In addition, the closer the initial guess is to the optimal solution, the faster the iteration.

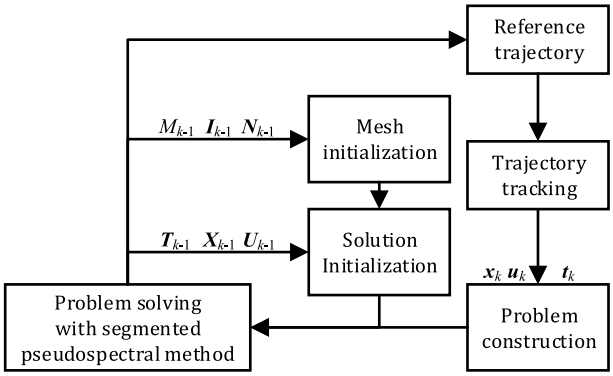

FIGURE 2. Framework of hierarchy-structure receding horizon optimization.

The framework of the receding horizon optimization is shown in Fig. 2. The exterior layer of the receding horizon optimization updates the reference trajectory according to the state feedback, and the process repeats over time. Therefore, the initial time and state constraints in each optimization are different. For the current state $\boldsymbol{x}_k$ of the kth cycle at the time t_k, the corresponding optimal control problem is denoted as $P_k(\boldsymbol{x}_k, t_k)$, which may be represented by (6). Then, the problem is solved by the segmented pseudospectral method. The obtained solution is a discrete set, $[\boldsymbol{X}_k, \boldsymbol{U}_k]$, that corresponds to the discrete-time series $\boldsymbol{T}_k$, where $\boldsymbol{X}_k$ denotes the state series, and $\boldsymbol{U}_k$ denotes the control series. Finally, a complete reference trajectory is generated by interpolating the discrete solution.

The inner layer of optimization solves the optimal control problem with new boundary constraints. The previous results are used as a priori information for the recursive initialization. The results include the discrete solution and mesh information. In general, the closer the initial value of the iteration is to the optimal solution, the shorter the solution time. Considering the case of no disturbance, the solutions of two adjacent optimizations are consistent but have different time ranges. Thus, it is desirable to interpolate

the previous solution to initialize the iteration. Note that the initial reference trajectory is derived from the off-board optimization.

The mesh information includes three parts: number of mesh intervals M, proportion of each interval, I, and degree of the approximating polynomial within each mesh interval, N. The degree of the polynomial is determined by the number of collocation points, and N can also denote the number of discrete points within each interval. Assuming the elements of vectors $\boldsymbol{I}$ and $\boldsymbol{N}$ are I and N, respectively, then their lengths are M and set $\sum \boldsymbol{I} = 1$.

For the kth cycle at time t_k, the terminal time in the previous solution is denoted as $t_{f,k-1}$, and the initialization of the mesh is given as follow:

(1) Locate the interval n, which satisfies

$$\boldsymbol{I}_{k-1}(1:n-1) \le (t_k - t_{k-1})/t_{f,k-1} < \boldsymbol{I}_{k-1}(1:n) \tag{7}$$

where ":" represents all elements from the start to the end position. Accordingly, the number of intervals is

$$M_k = M_{k-1} - n + 1 \tag{8}$$

(2) Update the proportion of each interval as follows:

$$\begin{aligned} \boldsymbol{I}_k(1) &= ((t_{f,k-1} - t_{k-1}) \sum \boldsymbol{I}_{k-1}(1:n) \\ &\quad + t_{k-1} - t_k)/(t_{f,k-1} - t_k) \\ \boldsymbol{I}_k(2:M_k) &= (t_{f,k-1} - t_{k-1})\boldsymbol{I}_{k-1} \\ &\quad \times (n+1:M_{k-1})/(t_{f,k-1} - t_k) \end{aligned} \tag{9}$$

(3) Update the number of discrete points. For the $\boldsymbol{N}_k(1)$, only the points after t_k in the interval n are retained, and for subsequent intervals, $\boldsymbol{N}_k(2{:}\,M_k) = \boldsymbol{N}_{k-1}(n+1{:}\,M_{k-1})$.

After the mesh is determined, the corresponding discrete time is obtained according to the total time interval $[t_0, t_f]$. When the iteration is initialized, let $t_{0=}t_k$, and $t_{f=}t_{f,k-1}$. The initial state series and control series corresponding to the initial time series are generated by the interpolation data, which includes the previous time series, state series, and control series.

The period of trajectory regeneration, T_r, is fixed in the proposed approach. However, during the receding horizon optimization, there may be situations where the solution does not converge or where the solution process is too long. Then the reference trajectory will not be updated until an acceptable solution is reached. The previous result is still used as the reference trajectory.

B. MODEL MODIFICATION

Model information is needed for both reference trajectory generation and trajectory tracking. The standard model is shown as (1). Due to the uncertainty of the model, the actual motion is inconsistent with the motion derived from the standard model. The uncertainties in thrust, aerodynamic coefficients, and atmospheric density have a considerable influence. To compensate for the uncertainties and reduce the difficulty of the trajectory tracking, three scale factors are introduced to modify the standard model, namely, the thrust scale factor K_T, lift scale factor K_L, and drag scale factor K_D. These three parameters can be estimated according to the overload coefficient measured by the accelerometer, which include the axial overload coefficient n_x and normal overload coefficient n_y. The observation model of scale factors is as follows:

$$\begin{bmatrix} n_x \\ n_y \end{bmatrix} = \begin{bmatrix} \frac{P}{mG_0} & -\frac{D}{mG_0}\cos\alpha & \frac{L}{mG_0}\sin\alpha \\ 0 & \frac{D}{mG_0}\sin\alpha & \frac{L}{mG_0}\cos\alpha \end{bmatrix} \begin{bmatrix} k_T \\ k_D \\ k_L \end{bmatrix} + \begin{bmatrix} \varepsilon_x \\ \varepsilon_y \end{bmatrix} \tag{10}$$

where ε_x and ε_y are the observation errors. The thrust, lift, and drag in (10) are calculated according to the standard model.

The above observation equation can be written as

$$\boldsymbol{Y} = \boldsymbol{H}\boldsymbol{\theta} + \boldsymbol{V} \tag{11}$$

where $\boldsymbol{Y}$ denotes the observation vector, $\boldsymbol{H}$ denotes the observation matrix, θ denotes the parameters to be estimated, and $\boldsymbol{V}$ denotes the observation errors.

Since the observation equation is linear, the parameters can be estimated effectively using the recursive least-squares method.

Define

$$\boldsymbol{P} = \left[\boldsymbol{H}^T\boldsymbol{H}\right]^{-1} \tag{12}$$

The estimation of parameters $\widehat{\boldsymbol{\theta}}$ at time t_j is calculated as

$$\widehat{\boldsymbol{\theta}}_j = \widehat{\boldsymbol{\theta}}_{j-1} + \boldsymbol{K}_{j-1}\left[\boldsymbol{Y}_j - \boldsymbol{H}_j\widehat{\theta}_{j-1}\right] \tag{13}$$

$$\boldsymbol{K}_{j-1} = \boldsymbol{P}_{j-1}\boldsymbol{H}_j^T\left[\boldsymbol{E} + \boldsymbol{H}_j\boldsymbol{P}_{j-1}\boldsymbol{H}_j^T\right]^{-1} \tag{14}$$

$$\boldsymbol{P}_j = \left[\boldsymbol{E} - \boldsymbol{K}_{j-1}\boldsymbol{H}_j\right]\boldsymbol{P}_{j-1} \tag{15}$$

where $\boldsymbol{E}$ denotes the identity matrix. The initial value of $\boldsymbol{P}$ and $\widehat{\theta}$ can be obtained by the least-squares method when the observed data exceeds than the number of parameters to be estimated.

The modified reference model is given as follows:

$$\begin{cases} \dot{v} = (K_T P\cos\alpha - K_D D)/m - g\sin\theta \\ \dot{\theta} = (K_T P\sin\alpha + K_L L)/(mv) - (g/v - v/(R_e + h))\cos\theta \end{cases} \tag{16}$$

The standard model is equivalent to the reference model with scale factors of 1. The parameter estimates are updated with new observations. As the observation data increases, the estimation accuracy will continue to be improved. Moreover, the modified model in trajectory tracking is kept consistent with the model used in trajectory regeneration.

C. TRAJECTORY TRACKING

Onboard optimization generates open-loop solutions. Due to the inaccuracies in modeling and external disturbance, the actual trajectory will constantly deviate from the reference trajectory. The active disturbance rejection control method can deal with model errors and unknown disturbance. Thus, it is used for control correction to track the reference trajectory which is continuously updated onboard. Moreover, the states concerned in the ascent phase include h, v, and θ, which represent the main feature of ascending. These three states are the object of trajectory tracking.

1) EXTENDED STATE OBSERVER

An extended state observer is designed for the multi-input and multi-output (MIMO) system. The observer is used to estimate the vehicle's state and the total disturbance that results from internal uncertainties and external disturbance. The real-time altitude h_c, velocity v_c, and mass of the vehicle are known. Then, the nonlinear observer can be designed as

$$\begin{cases} e_1 = z_1 - h_c \\ e_2 = z_2 - v_c \\ e_3 = (\beta_0 e_1 - e_2 \sin z_3)/z_2 \cos z_3 \\ \dot{z}_1 = z_2 \sin z_3 - \beta_1 e_1 - e_2 \sin z_3 \\ \dot{z}_2 = f_v(z_1, z_2, z_3, \boldsymbol{u}) + z_4 - \beta_2 e_2 \\ \dot{z}_3 = f_\theta(z_1, z_2, z_3, \boldsymbol{u}) + z_5/v - \beta_3 e_3 \\ \dot{z}_4 = -\beta_4 fal(e_2, \omega_v, \delta_0) \\ \dot{z}_5 = -\beta_5 fal(e_3, \omega_\theta, \delta_0) \end{cases} \tag{17}$$

where β_0, β_1, β_2, β_3, β_4, β_5 are observer gains to be designed; z_1, z_2, z_3 denote the estimated values of h, v, θ, respectively; z_4, z_5 denote the estimated values of total disturbances resulting from inaccurate modeling and unknown disturbances; $f_v(z_1, z_2, z_3, \boldsymbol{u})$ and $f_\theta(z_1, z_2, z_3, \boldsymbol{u})$ denote the modeled accelerations, which are calculated according to the reference model shown in (16); and $0 < \omega_v, \omega_\theta < 1$, δ_0 is a tiny positive constant to limit the neighborhood of the origin.

The nonlinear function $fal(e, \omega, \delta)$ is given as

$$fal(e, \omega, \delta) = \begin{cases} e/\delta^{1-\omega}, \|e\| \le \delta \\ \mathrm{sgn}(e) e^{\omega}, \|e\| > \delta \end{cases} \tag{18}$$

where $\mathrm{sgn}(e)$ denotes the sign of variable e.

2) LINEARIZATION WITH DYNAMIC COMPENSATION

To facilitate the derivation of the feedback control law, define two accelerations as follows:

$$a_v = (K_T P \cos\alpha - K_D D)/m, a_\theta = (K_T P \sin\alpha + K_L L)/m \tag{19}$$

The strong coupling between the thrust and aerodynamics makes it difficult to correct the AOA and throttle coefficient directly. However, the two accelerations, a_v and a_θ, can be corrected directly according to the feedback. The original dynamic system is linearized based on compensating the time-varying disturbances estimated by the extended state observer. The new virtual control variables may be defined as follows

$$\begin{cases} u_1' = a_v + z_4 - g \sin z_3 \\ u_2' = a_\theta + z_5 - (g - z_2^2/(R_e + z_1)) \cos z_3 \end{cases} \tag{20}$$

The original system is transformed into

$$\begin{cases} \dot{h} = v \sin\theta \\ \dot{v} = u_1' \\ \dot{\theta} = u_2'/v \end{cases} \tag{21}$$

For the above system, the reference state tracking law is designed as follows:

$$\begin{cases} u_1' = \dot{v}_{\mathrm{ref}} + \kappa_{v1} fal(v_{\mathrm{ref}} - z_2, \omega_{v1}, \delta_1) \\ \qquad + \kappa_{v2} fal(h_{\mathrm{ref}} - z_1, \omega_{v1}, \delta_1) \\ u_2' = (\dot{\theta}_{\mathrm{ref}} + \kappa_{\theta 1} fal(\theta_{\mathrm{ref}} - z_3, \omega_{\theta 1}, \delta_2) \\ \qquad + \kappa_{\theta 2} fal(h_{\mathrm{ref}} - z_1, \omega_{\theta 2}, \delta_2)) z_2 \end{cases} \tag{22}$$

where κ_{v1}, κ_{v2}, $\kappa_{\theta 1}$, $\kappa_{\theta 2}$ are feedback gains to be designed. Subscript "ref" denotes the reference state.

The accelerations a_v and a_θ can be calculated by u_1' and u_2', respectively. Then, the guidance command $[\phi_t, \alpha]^T$ is obtained by solving the equations in (19), and the command is limited by the path constraints.

TABLE 1. Boundary constraints.

Symbol	Description	Value
H_0(km)	Initial altitude	0
v_0(m•s^{-1})	Initial velocity	80
θ_0(°)	Initial path angle	0
m_0(kg)	Initial mass	128000
H_f(km)	Terminal altitude	45
v_f(Ma)	Terminal velocity	8
θ_f(°)	Terminal path angle	0

IV. NUMERICAL SIMULATIONS

In simulations, the vehicle takes off horizontally and then climbs to the expected altitude to cruise in near-space conditions at hypersonic velocity. This scenario is applied to a two-stage-to-orbit space plane and hypersonic aircraft. The parameters used in the simulations are shown in Table 1 and Table 2.

The observer gains in the simulation are set as: $\beta_0 = \beta_1 = \beta_2 = \beta_3 = 5$, and $\beta_4 = \beta_5 = 100$. Parameters of function fal are: $\omega_v = \omega_\theta = 0.5$, and $\delta_0 = 0.2$.

TABLE 2. Path constraints.

Symbol	Description	Value
α (°)	Range of AOA	[-3 21]
$\dot{\alpha}$ (°·s^{-1})	Range of the derivative of AOA	[-1 1]
ϕ_t	Range of throttle coefficient	[0 2]
$\dot{\phi}_t$ (s^{-1})	Range of the derivative of throttle coefficient	[-0.1 0.1]
q_{max} (kPa)	Upper bound of dynamic pressure	350

TABLE 3. Bias of parameters in the simulation.

Symbol	Description	Value
$\Delta\rho$ (%)	Relative bias of atmospheric density	-30
ΔC_L (%)	Relative bias of lift coefficient	30
ΔC_D (%)	Relative bias of drag coefficient	30
ΔI_{sp} (%)	Relative bias of specific impulse	-5

The simulation has two parts. The first part involves verifying the effectiveness of the guidance method. In the second part, the robustness of the method is further discussed. The computation is performed on a laptop with a Core i7-4712M 2.30-GHz CPU. The solutions of trajectory optimization are obtained via the solver SPTOS developed by our group.

A. EFFECTIVENESS

To assess the efficiency of the proposed method, the proposed method is compared with the trajectory tracking guidance without trajectory regeneration. The bias resulting in the simulation from the specific impulse, atmospheric density, and aerodynamic coefficients are listed in Table 3.

The onboard trajectory regeneration cycle T_r is set as 5s. As shown in Fig. 3, guidance without trajectory regeneration cannot satisfy the requirement. This is due to the limited correction ability of the trajectory tracker. The reference throttle coefficient remains at the maximum, and the acceleration capacity reaches the upper limit. Therefore, it is difficult to achieve the nominal trajectory by adjusting the AOA alone. The trajectory regeneration can adaptively update the reference state and control command according to the state feedback. The receding horizon optimization realizes the iterative update of reference trajectory, and the vehicle can ascend with less fuel consumption while satisfying the boundary constraints and path constraints. The terminal altitude error is 0.014 m, the terminal path angle error is less than 0.001°, and the velocity error is -0.243 m·s^{-1}. The method can adapt to the changes of the multi-modal complex

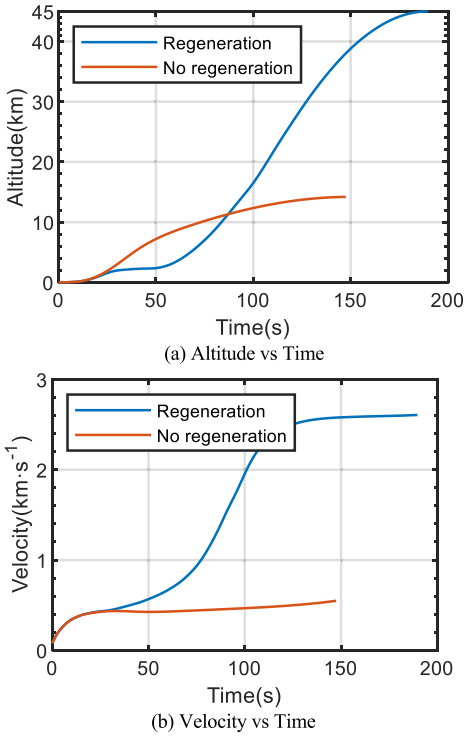

FIGURE 3. Altitude and velocity.

system, and the guidance accuracy with the large deviation is satisfactory.

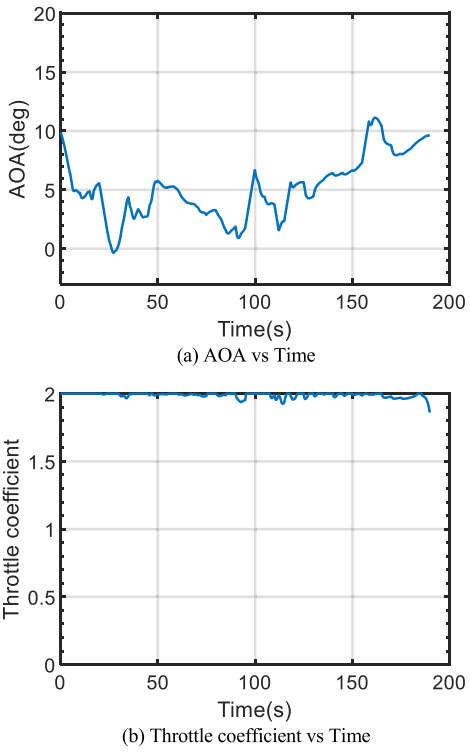

FIGURE 4. Control variables.

Fig. 4 shows the control variables during the ascent phase, and Fig. 5 shows the time history of dynamic pressure.

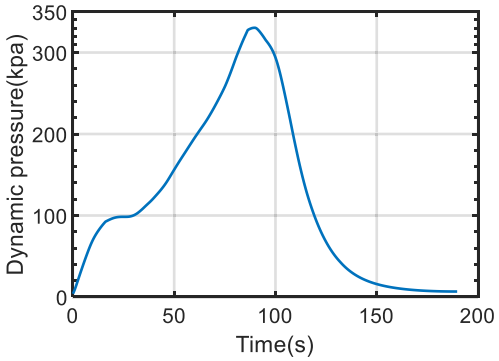

FIGURE 5. Dynamic pressure.

The path constraints of the control and dynamic pressure are satisfied. The reference guidance command is updated by receding horizon optimization and then corrected by the trajectory tracker. The control changes differently in different engine modalities and environments, even as the focus remains on lowering the fuel consumption. The acceleration takes precedence over the increase in altitude, as the relatively higher atmospheric density at low altitude means that less fuel is needed to accelerate the vehicle. After approaching the desired velocity, the vehicle arrives at the expected altitude mainly by adjusting the AOA. The throttle coefficient is adjusted so that the velocity changes smoothly. The model modification improves the adaptability of the method, making the reference trajectory closer to the actual situation. The influence of model deviation is weakened, which may result in the failure of the trajectory regeneration.

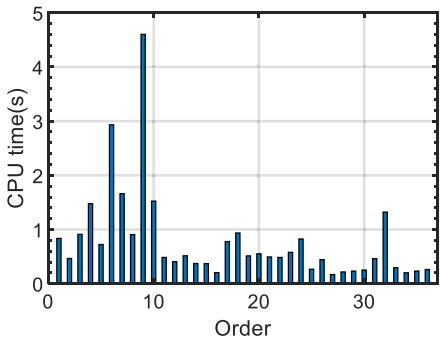

FIGURE 6. CPU times of onboard trajectory optimization.

Fig. 6 shows the CPU times of each reference trajectory optimization. Most of the calculation times are less than 0.5s, and all the calculation times are less than the duration of the regeneration cycle. In the inner layer of receding horizon optimization, the recursive initialization makes the segmented pseudospectral method converge quickly to the optimal solution. As mentioned above, the receding horizon optimization with recursive initialization iteratively updates the reference trajectory. Although the calculation models used for adjacent optimizations are different, the convergence from the previous reference trajectory to the new optimal solution is rapid enough, and fast calculation is conducive to onboard application.

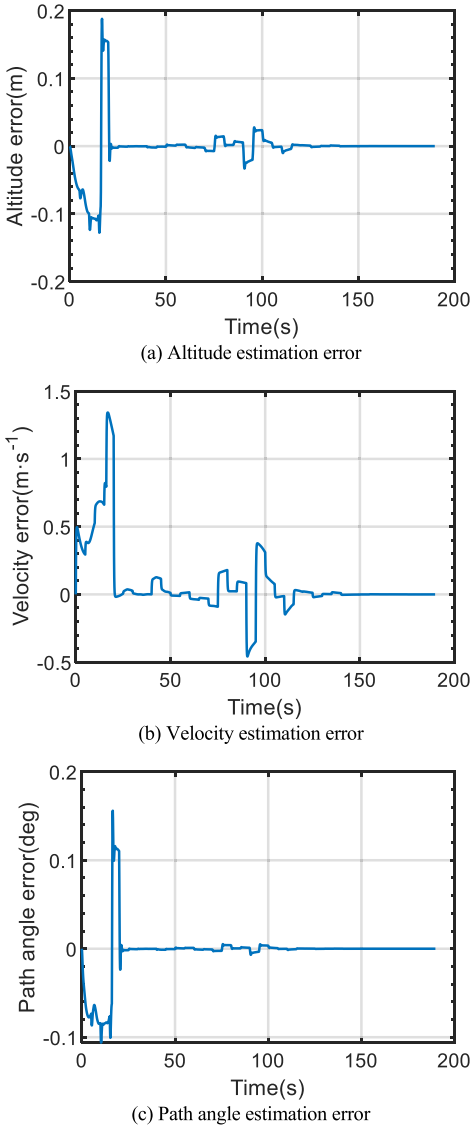

FIGURE 7. Estimation errors.

The extended state observer with model modification can estimate the state of the vehicle accurately. Fig. 7 shows the estimation errors of the extended state observer. The errors gradually converge to near zero. The altitude estimation error is more sensitive to the path angle error as their trends are close and similar. The error changes discontinuously with the model modification, but the modification reduces the pressure on the state observer.

B. ROBUSTNESS

Furthermore, different deviations are applied to validate the robustness of the guidance method. The bias conditions are shown in Table. 4.

TABLE 4. Bias condition for determining robustness.

Symbol	Description	Value
$\Delta\rho$ (%)	Relative bias of atmospheric density	±30
ΔC_L , ΔC_D (%)	Relative bias of aerodynamic coefficient	±30
ΔI_{sp} (%)	Relative bias of specific impulse	±5

TABLE 5. The terminal errors.

Sign	Altitude error(m)	Velocity error(m•s^{-1})	Path angle error(deg)
(−,+,−)	0.014	-0.243	0.001
(−,+,+)	-0.081	-0.714	0.030
(+,+,+)	-0.007	-0.478	0.066
(+,+,−)	-0.019	-0.461	0.042
(−,−,+)	-0.052	-0.609	0.042
(−,−,−)	-0.086	-0.270	0.025
(+,−,+)	-0.153	-0.720	0.047
(+,−,−)	-0.023	-0.578	0.006

TABLE 6. Results with different regeneration cycles.

Regeneration cycle(s)	Altitude error(m)	Velocity error(m•s^{-1})	Path angle error(deg)
5	0.014	-0.243	0.001
10	-0.046	-0.403	0.079
15	0.477	-0.481	0.011

There are eight combinations of extreme bias conditions. $(-, +, +)$ is used to denote the sign of each bias. The terminal errors in these cases are shown in Table 5.

All results meet the constraints. The terminal errors demonstrate the robustness of the proposed method. The trajectory tracker based on ADRC is supplemented by the model modification to ensure that the guidance method can cope with the disturbance.

In fact, the terminal guidance accuracy is affected directly by the last onboard trajectory regeneration. Once the reference trajectory is successfully updated when the vehicle approaches the terminal state, the error in trajectory tracking remains within acceptable limits. Thus high guidance accuracy can be achieved. Table 6 shows the simulation results with different regeneration cycles for the same bias condition as in Table 3. As the regeneration cycles proceed, the terminal accuracy decreases, but all the errors are accepted. This implies that even if there are several reference regeneration failures during the ascent, the guidance will not fail, and the terminal guidance accuracy can still be high.

V. CONCLUSION

A novel guidance method for a vehicle with a combined cycle engine is proposed in this paper. The onboard trajectory planning and reference trajectory tracking are examined. For onboard trajectory planning, a hierarchical receding horizon optimization algorithm is designed and the reference trajectory is updated iteratively according to the state feedback. The recursive initializations of both the discrete mesh and the iterative solution are introduced in the segmented pseudospectral optimization to solve the optimal control problem quickly. Then, based on the ADRC theory, an extended state observer is designed for the MIMO system. The disturbance is estimated according to the system output and compensated in model linearization to improve the robustness of trajectory tracking. Finally, to match the optimal result to the actual situation and make it easier to track the reference trajectory, three scale factors are defined to modify the models. The recursive least-square method is used to estimate the three factors. Model modification and ADRC complement each other to ensure the overall robustness of the guidance. Simulation results indicate the efficiency of the proposed ascent guidance method. The method can meet the requirements of adaptability and robustness. Besides, the guidance based on onboard trajectory regeneration can also provide a general solution applicable to the ascent guidance for vehicles.

REFERENCES

[1] S. R. Thomas, J. F. Walker, and J. L. Pittman, "Overview of the turbine based combined cycle discipline," NASA, Washington, DC, USA, Tech. Rep. 20110012002, Sep. 2009.

[2] H. Taguchi, H. Futamura, K. Shimodaira, T. Morimoto, T. Kojima, and K. Okai, "Design study on hypersonic engine components for TBCC space planes," in *Proc. 12th AIAA Int. Space Planes Hypersonic Syst. Technol.*, Norfolk, VA, USA, Dec. 2003, pp. 1–10.

[3] Z.-W. Huang, G.-Q. He, F. Qin, R. Xue, X.-G. Wei, and L. Shi, "Combustion oscillation study in a kerosene fueled rocket-based combined-cycle engine combustor," *Acta Astronaut.*, vol. 129, pp. 260–270, Dec. 2016, doi: 10.1016/j.actaastro.2016.09.024.

[4] Z. Dong, M. Sun, Z. Wang, J. Chen, and Z. Cai, "Survey on key techniques of rocket-based combined-cycle engine in ejector mode," *Acta Astronaut.*, vol. 164, pp. 51–68, Nov. 2019, doi: 10.1016/j.actaastro.2019.07.016.

[5] F.-Y. Zuo and S. Mölder, "Hypersonic wavecatcher intakes and variable-geometry turbine based combined cycle engines," *Prog. Aerosp. Sci.*, vol. 106, pp. 108–144, Apr. 2019, doi: 10.1016/j.paerosci.2019.03.001.

[6] P. Klink and H. Ogawa, "Investigation on the performance and feasibility of RBCC-based access-to-space via multi-objective design optimization," *Acta Astronaut.*, vol. 157, pp. 435–454, Apr. 2019, doi: 10.1016/j.actaastro.2018.12.034.

[7] H. Zhou, X. Wang, Y. Bai, and N. Cui, "Ascent phase trajectory optimization for vehicle with multi-combined cycle engine based on improved particle swarm optimization," *Acta Astron.*, vol. 140, pp. 156–165, Nov. 2017, doi: 10.1016/j.actaastro.2017.08.024.

[8] K. D. Mease and M. A. Van Buren, "Geometric synthesis of aerospace plane ascent guidance logic," *Automatica*, vol. 30, no. 12, pp. 1839–1849, Dec. 1994, doi: 10.1016/0005-1098(94)90046-9.

[9] L. Zhou and L. Yin, "Dynamic surface control based on neural network for an air-breathing hypersonic vehicle," *Optim. Control Appl. Methods*, vol. 36, no. 6, pp. 774–793, Aug. 2014, doi: 10.1002/oca.2130.

[10] X. Hu, C. Hu, L. Wu, and H. Gao, "Output tracking control for nonminimum phase flexible air-breathing hypersonic vehicle models," *J. Aerosp. Eng*, vol. 28, no. 2, pp. 1–44, Sep. 2013, doi: 10.1061/(ASCE)AS.1943-5525.0000383.

[11] V. Brinda, S. Dasgupta, and M. Lal, "Trajectory optimization and guidance of an air breathing hypersonic vehicle," in *Proc. 14th AIAA/AHI Space Planes Hypersonic Syst. Technol. Conf.*, Canberra, ACT, Australia, Nov. 2006, pp. 856–869, doi: 10.2514/6.2006-7997.
[12] G. D. Zhu and Z. J. Shen, "Three dimensional trajectory linearization control for flight of air-breathing hypersonic vehicle," *Proc. Eng.*, vol. 99, pp. 268–279, Jan. 2015, doi: 10.1016/j.proeng.2014.12.535.
[13] J. T. Betts, "Survey of numerical methods for trajectory optimization," *J. Guid., Control, Dyn.*, vol. 21, no. 2, pp. 193–207, Mar. 1998, doi: 10.2514/2.4231.
[14] B. A. Conway, "A survey of methods available for the numerical optimization of continuous dynamic systems," *J. Optim. Theory Appl.*, vol. 152, no. 2, pp. 271–306, Feb. 2012, doi: 10.1007/s10957-011-9918-z.
[15] P. Lu, H. Sun, and B. Tsai, "Closed-loop endoatmospheric ascent guidance," *J. Guid., Control, Dyn.*, vol. 26, no. 2, pp. 283–294, Mar. 2003, doi: 10.2514/2.5045.
[16] M. H. Gräßlin, J. Telaar, and U. M. Schöttle, "Ascent and reentry guidance concept based on NLP-methods," *Acta Astronaut.*, vol. 55, nos. 3–9, pp. 461–471, Aug. 2004, doi: 10.1016/j.actaastro.2004.05.004.
[17] T. Yamamoto and J. Kawaguchi, "A new real-time guidance strategy for aerodynamic ascent flight," *Acta Astronaut.*, vol. 61, nos. 11–12, pp. 965–977, Dec. 2007, doi: 10.1016/j.actaastro.2006.12.026.
[18] O. Murillo and P. Lu, "Fast ascent trajectory optimization for hypersonic air-breathing vehicles," in *Proc. AIAA Guid., Navigat., Control Conf.*, Toronto, ON, Canada, Aug. 2010, pp. 1–24.
[19] L. Xie, H. Zhang, X. Zhou, and G. Tang, "A convex programming method for rocket powered landing with angle of attack constraint," *IEEE Access*, vol. 8, pp. 100485–100496 2020, doi: 10.1109/ACCESS.2020.2997235.
[20] D. Zhang, L. Liu, and Y. Wang, "On-line ascent phase trajectory optimal guidance algorithm based on pseudo-spectral method and sensitivity updates," *J. Navigat.*, vol. 68, no. 6, pp. 1056–1074, Jun. 2015, doi: 10.1017/S0373463315000326.
[21] X. Lu, Y. Wang, and L. Liu, "Optimal ascent guidance for air-breathing launch vehicle based on optimal trajectory correction," *Math. Problems Eng.*, vol. 2013, pp. 1–11, Oct. 2013, doi: 10.1155/2013/313197.
[22] H. Zhou, X. Wang, W. Shan, and N. Cui, "Ascent guidance law for a horizontal take-off vehicle with a multi-combined cycle engine," *Adv. Space Res.*, vol. 65, no. 1, pp. 379–391, Jan. 2020, doi: 10.1016/j.asr.2019.10.008.
[23] *U.S. Standard Atmosphere*, U.S. Government Printing Office, Washington, DC, USA, 1976.
[24] O. J. Murillo, "A fast ascent trajectory optimization method for hypersonic air-breathing vehicles," Ph.D. dissertation, Dept. Aerosp. Eng., Iowa State Univ, Ames, IA, USA, 2010.
[25] M. A. Patterson, W. W. Hager, and A. V. Rao, "A ph mesh refinement method for optimal control," *Optim. Control Appl. Methods*, vol. 36, no. 4, pp. 398–421, Aug. 2015, doi: 10.1002/oca.2114.
[26] W. W. Hager, H. Hou, S. Mohapatra, A. V. Rao, and X.-S. Wang, "Convergence rate for a Radau hp collocation method applied to constrained optimal control," *Comput. Optim. Appl.*, vol. 74, no. 1, pp. 275–314, May 2019.

XIANGJI TANG received the B.S. degree in aeronautics and astronautics science and technology from BUAA, in 2019. He is currently pursuing the M.S. degree in aeronautics and astronautics science and technology with the National University of Defense Technology. His research interests include real time trajectory optimization and flight vehicle dynamics and guidance.

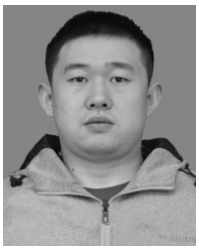

ZHAOTING LI received the M.S. degree in aeronautics and astronautics science and technology from the National University of Defense Technology, Changsha, China, in 2018, where he is currently pursuing the Ph.D. degree in aeronautics and astronautics science and technology. His research interests include trajectory optimization, and flight vehicle dynamics, guidance, and control.

HONGBO ZHANG received the Ph.D. degree in aeronautics and astronautics from the National University of Defense Technology, in 2009. He is currently a Professor and a Master Tutor with the College of Aerospace Science and Engineering, National University of Defense Technology. His research interests include orbit dynamics and control, flight vehicle dynamics and control, and entry guidance.